UDC 54 DOI: 10.18698/1812-3368-2023-4-175-193

PREPARATION AND CHARACTERIZATION OF BIOCOMPOSITE FILMS OF SODIUM ALGINATE/KAPPA-CARRAGEENAN/IOTA-CARRAGEENAN LOADED WITH AMINOETHOXYVINYLGLYCINE

N.A. Villacrés[1] nvillacresm@uni.pe
É.T.G. Cavalheiro[2] cavalheiro@iqsc.usp.br
A.P.G. Ferreira[2] anagarcia@iqsc.usp.br
T. Venâncio[3] venancio@ufscar.br
H.A. Alarcón[1] halarcon@uni.edu.pe
A.C. Valderrama[1] ana.valderrama.n@uni.edu.pe

[1] **National University of Engineering, Lima, Peru**
[2] **University of São Paulo, São Paulo, Brazil**
[3] **Federal University of São Carlos, São Paulo, Brazil**

Abstract

This work focused on the development of a new biomaterial from polysaccharides. Thus composite films of sodium alginate, κ-carrageenan, and ι-carrageenan plasticized with glycerol and poly(ethylene glycol) 400 (PEG 400) were prepared. The surface properties of the resulting films in terms of surface morphology were investigated. The best ratio between glycerol and PEG 400 used as plasticizers to prepare sodium alginate films was determined. Opacity, water content, SEM, TGA, and FTIR studies determined the optimal ratio between glycerol and PEG 400. The addition of carrageenans in the composite films showed differences in the TGA curves and on surface of the films. The composite film was loaded with an ethanolic solution of aminoethoxyvinylglycine (AVG). The AVG loaded in the composite film exhibited improved surface area, increased percent of crystallinity, and higher percent release at a lower temperature and its release kinetics were studied

Keywords

Alginate, carrageenan, plasticizers, films, aminoethoxyvinylglycine

Received 16.02.2023
Accepted 07.04.2023

The research was funded by the Peruvian government through Prociencia/World Bank Program (project grant 01-2018-FONDECYTBM-IADTUM)

Introduction. The environmental pollution generated by dumping and accumulating synthetic plastics has created the need to develop biodegradable

materials [1]. These materials, called biopolymers, are prepared from renewable sources such as polysaccharides, proteins, and mixtures [2].

Polysaccharides are used to produce biopolymers due to their highwater retention, non-toxicity, biocompatibility, and ability to act as drug carriers [3]. The mixture of polysaccharides is used to improve the physicochemical properties of biopolymers, obtain films with functional activities [4], and design controlled and sustained release formulations [5]. Among the various polysaccharides, the most used are cellulose, starch, chitosan, alginate, and carrageenan [6].

Sodium alginate is a water-soluble, biodegradable, and biocompatible polysaccharide extracted from brown algae and composed of linear (1–4) bonds of α-L-guluronic acid and β-D-mannuronic acid [7] (Fig. 1, *a*). Due to its good mechanical resistance, this polysaccharide is used to produce edible films and coatings. However, it is highly soluble in water [8], limiting its application in food packaging [9].

Carrageenans are polysaccharides extracted from red algae. Chemically, carrageenans are considered as the partially sulfated galactans [10]. They are formed by a linear backbone of repeating units of D-galactose and 3,6-anhydro-D-galactose (3,6-AG) linked through alternating α-(1-3) and β-(1-4) glycosidic [11], which allows them to be used in the production of biodegradable films [12]. The number and position of the sulfate ester groups and the 3,6-AG content allow carrageenan to be classified into λ (lambda), κ (kappa), ι (iota), υ (nu), μ (mu), θ (theta) and ξ (xi). For example, kappa-carrageenan (κ-carrageenan) has a sulfate group at O-4 of β-D-galactopyranose (Fig. 1, *b*), which contains 25–30 % sulfate ester and 28–35 % 3,6-AG, and iota-carrageenan (ι-carrageenan) has an additional sulfate group residue at O-2 of α-D-galactopyranose (Fig. 1, *c*) and contains 28–35 % sulfate ester and 25–30 % 3,6-AG [13].

Plasticizers are low molecular weight, non-volatile, and high boiling liquid additives. They are used to increase the flexibility or plasticity of polymers and to facilitate the processing of polymeric films [14]; commonly used plasticizers include glycerol, sorbitol, polyethylene glycol, xylitol, and urea [15]. Glycerol is a non-volatile polyol used as a plasticizer because it increases the mechanical and permeability properties of the films; due to the hydrogen bonds between the polymer chains that expand the intermolecular spaces and lead to an increase in the permeability and flexibility of the films [16]. Polyethylene glycol (PEG) is commercially available in a wide range of molecular weights, from 300 to 10,000 $g \cdot mol^{-1}$, and due to its excellent biocompatibility and non-toxicity, it is used in film production. The increase in the molecular weight of PEG causes

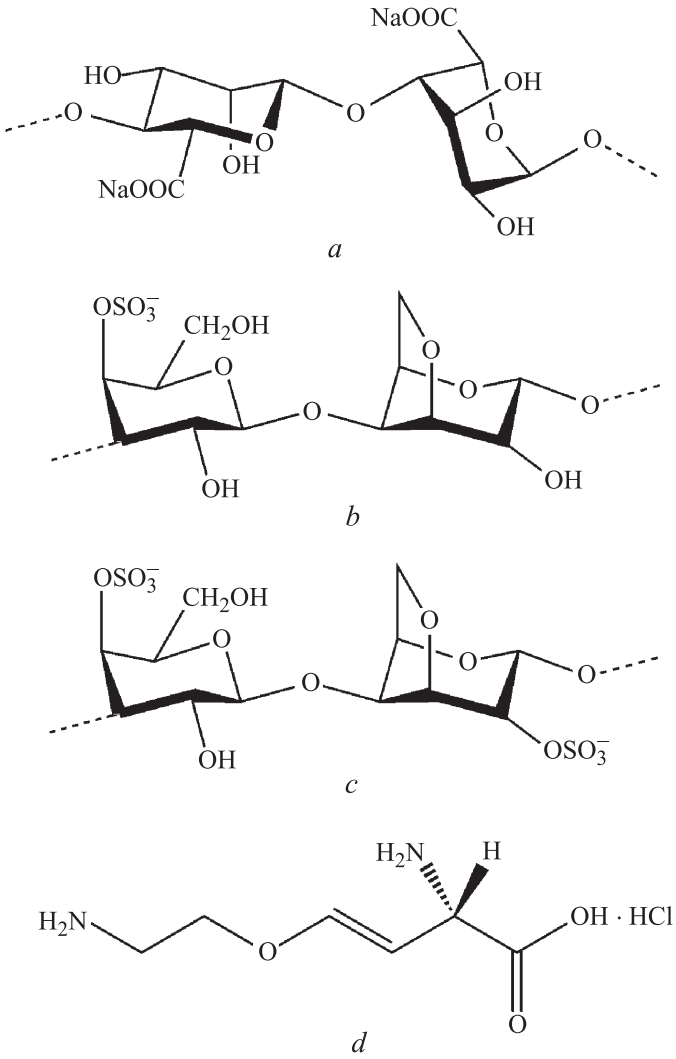

Fig. 1. Structural representation of sodium alginate (*a*), κ-carrageenan (*b*), ι-carrageenan (*c*) and structural formula of aminoethoxyvinylglycine (*d*)

a decrease in its polarity and solubility, as well as its ability to interact with polymer chains, so PEGs with lower molecular weights exhibit a better plasticizing effect [17]. When the plasticizer is added to aqueous polymer dispersion, it disperses within the aqueous phase and diffuses between the polymeric matrices. However, when a mixture of polymers is present, its distribution within the coating dispersions and films may not be homogeneous [18].

The films made with polysaccharides are loaded with different active agents because these substances can migrate from the material to the food [19]. These films can be loaded with ethylene inhibitors and used to prevent the negative

effects caused by the ripening process induced by ethylene in foods, prolonging the shelf life of foods [20]. Ethylene inhibitors are classified as biosynthesis inhibitors, e.g., aminoethoxyvinylglycine (AVG), and action inhibitors, e.g., 1-methyl-cyclopropene (1-MCP) [21]. Aminoethoxyvinylglycine — AVG ((S)-trans-2-amino-4-(2-aminoethoxy)-3-butenoic acid hydrochloride) (Fig. 1, *d*) is an ethoxy analog of rhizobitoxine that inhibits ethylene biosynthesis by blocking the action of the 1-aminocyclopropane-1-carboxylic acid synthase enzyme [22].

Considering the need and importance of the development of new materials made from natural resources, this research focused on the study of the proportion between plasticizers and the addition of carrageenan derivatives in a sodium alginate solution to prepare composite films loaded with an ethylene inhibitor and study its release kinetics.

Materials. Sodium alginate, glycerol 99 % GC, average weight poly(ethylene glycol) Mn 400 (PEG 400), κ-carrageenan (sulfated plant polysaccharide), ι-carrageenan (commercial grade, type II, predominantly iota carrageenan) and aminoethoxyvinylglycine hydrochloride were purchased from Sigma — Aldrich. Ethanol from Merck was also used.

Experimental methods and analysis. *Preparation of composite films loaded with AVG.* The preparation of the composite films loaded was performed in three stages. In the first stage, the relationship between plasticizers (glycerol and PEG 400) and sodium alginate in the production of films was determined; in the second stage, composite films of sodium alginate with κ-carrageenan and ι-carrageenan were prepared, and in the third stage the composite film loaded with AVG was prepared. Table 1 details the parameters used in the preparation of the films.

Table 1

Parameters used in the preparation of the films

Film	[NaAlg], mL	Glycerol, g	PEG-400, g	[κ-carrageenan], mL	[ι-carrageenan], mL	AVG, mL
NaAlgCG9P1	30	0.9	0.1	–	–	–
NaAlgCG7P3		0.7	0.3			
NaAlgCG5P5		0.5	0.5			
NaAlgCG9P1k		0.9	0.1	5.0		
NaAlgCG9P1i				–	5.0	–
NaAlgCG9P1ki				5.0		
NaAlgCG9P1kiA						10

Determination of the ratio of plasticizers. In this case 30 mL of 1.5 % $w \cdot v^{-1}$ sodium alginate (NaAlg) and 1 g of glycerol and poly(ethylene glycol) (PEG 400) mixture in different ratios (9:1, 7:3, and 5:5 $w \cdot w^{-1}$; respectively) was prepared. These solutions were kept under constant stirring for 30 minutes at 50 °C and poured into Petri dishes, and dried at 50 °C for 24 h.

Addition of carrageenans. Thus, 30 mL of sodium alginate (NaAlg) at 1.5 % $w \cdot v^{-1}$ was mixed with 5 mL of κ-carrageenan (1.0 % $w \cdot v^{-1}$) and/or 5 mL of ι-carrageenan (1.0 % $w \cdot v^{-1}$) and kept under constant stirring for 60 min at 70 °C. Then 1 g of the mixture of glycerol and PEG 400 in a 9:1 $w \cdot w^{-1}$ ratio was added and stirred for 30 min at 50 °C. Finally, the solutions were molded into a petri dish and dried at 50 °C for 24 h.

Loaded AVG. In this case 30 mL of sodium alginate (NaAlg) at 1.5 % $w \cdot v^{-1}$ was mixed with 5 mL of κ-carrageenan (1.0 % $w \cdot v^{-1}$) and 5 mL of ι-carrageenan (1.0 % $w \cdot v^{-1}$) for 60 min at 70 °C. Then 1 g of the mixture of glycerol and PEG 400 in a 9:1 $w \cdot w^{-1}$ ratio was added to the mixture of polysaccharides and stirred for 30 minutes at 50 °C. Subsequently, 10 mL of an ethanolic solution of aminoethoxyvinylglycine (AVG) (20 $mg \cdot L^{-1}$) was added and for 30 min at 50 °C was stirred. Finally, the solution was poured into a petri dish and dried at 50 °C for 24 h.

AVG Release. The loaded films were immersed in 25 mL of a 70 % ethanolic solution with constant stirring at 100 RPM at 10 and 25 °C. For measurement purposes, 2 ml of release medium were withdrawn at predetermined times, and its absorbance was measured at 197.5 nm using a UV-1800 UV-V is spectrophotometer (Shimadzu). This aliquot was returned after each reading, and the system was kept under stirring until the next reading.

To evaluate whether Fick's law governs the diffusion processes, the equations of Higuchi [23]

$$\frac{M_t}{M_\infty} = K_H t^{0.5}, \tag{1}$$

and Korsmeyer — Peppas [24]

$$\frac{M_t}{M_\infty} = K t^n \tag{2}$$

were used. These equations describe the release process from one of the faces of the film and the release from erosion or dissolution of the polymeric matrix, respectively. In Eq. (1), (2) M_t / M_∞ is the fraction of solute released at time t, K_H is the Higuchi diffusion constant. In Eq. (2) K is the system constant, n is the diffusion exponent.

Opacity. The opacity of the films containing different proportions in the mixture of plasticizers was obtained using equation

$$Opacity = \frac{-\log T}{d},$$

where T is the light transmittance of the film at 600 nm; d is the thickness of the film (mm).

Film thickness images were collected using a *Zeiss-LSM780* laser scanning microscope with an inverted confocal fluorescence, 40× objective lens, a numerical aperture of 0.8, and a resolution at *x* of *rx* = 165 nm, and using the *ImageJ* software, the thickness value was obtained by taking 10 measurements. In addition, the transmittance value was recorded on *Varian Cary*® 50 UV-Vis spectrophotometer.

Water content. The water content of the films made with different proportions of glycerol and PEG 400 was obtained by cutting the films into rectangular pieces and then weighing them before and after being dried at 105 °C for 24 h in an oven

$$Water\,content = \frac{W_i - W_f}{W_f},$$

where W_i, W_f are the initial (g) and the final masses of the film (g). Water content was expressed as g (H_2O) g^{-1} (dry solids).

Characterization. *Fourier transform infrared (FTIR)*. FTIR spectra were obtained on the *Shimadzu IRPrestige 2*1 spectrophotometer with attenuated total reflectance (ATR) module.

Thermogravimetric analysis (TGA). The thermogravimetric curves were collected in a SDT Q600 simultaneous TG/DTA modulus managed by the Thermal Advantage for Q Series software (v. 5.5.24) both from TA Instruments. Measurements were performed in open α-alumina sample holders using sample mass of 5.0 ± 0.1 mg in a dynamic N_2 atmosphere flowing at 50 mL · min^{-1}; the temperature range was selected as 25–1000 °C with a heating rate of 10 °C · min^{-1}.

X-ray diffraction (XRD). The diffractograms were obtained in a range of 2θ from 5° to 100° in a D8 Advance diffractometer equipment (Brüker) equipped with a Cu source (Kα = 1.5418 Å) operating at a voltage of 40 kV and 40 mA (1600 W) and a *LynxEye* model PSD type detector.

Scanning electron microscopy (SEM). Images were obtained with an LEO 440 microscope (Cambridge) equipped with a 7060 detector (Oxford) and

at resolutions of 10 and 1 μm at 1000× and 5000× magnification, respectively. The samples were gold-plated in a MED 020 high vacuum metallizer (Bal-Tec).

Results and discussions. ***Preparation of films.*** *First stage.* Three films of sodium alginate plasticized with a mixture of glycerol and PEG 400 at different proportions were prepared: the first film was named NaAlgCG9P1 (Fig. 2, *a*), the second film NaAlgCG7P3 (Fig. 2, *b*), and the third film NaAlgCG5P5 (Fig. 2, *c*). The increase of PEG 400 in the ratio of the plasticizers increased the opacity (Table 2), decreased the percentage of transmittance at 600 nm, and modified the surface of the films, making them rougher (Fig. 2, *d–f,* Fig. 3, *a*). The whitish appearance of the films may be due to the high molecular weight and relatively low content of hydroxyl groups of PEG 400, which caused phase separation and incompatibility with the NaAlg polymeric matrix and increased surface roughness and heterogeneity of the films [25]. On the contrary, glycerol has a greater number of polar groups (–OH), which generates an increase in the moisture content in the films (see Table 2), and greater compatibility by forming hydrogen bonds with the hydroxyl groups of NaAlg [26], which creates large spaces between the polymer chains and improves the homogeneity on the surface of the films [27].

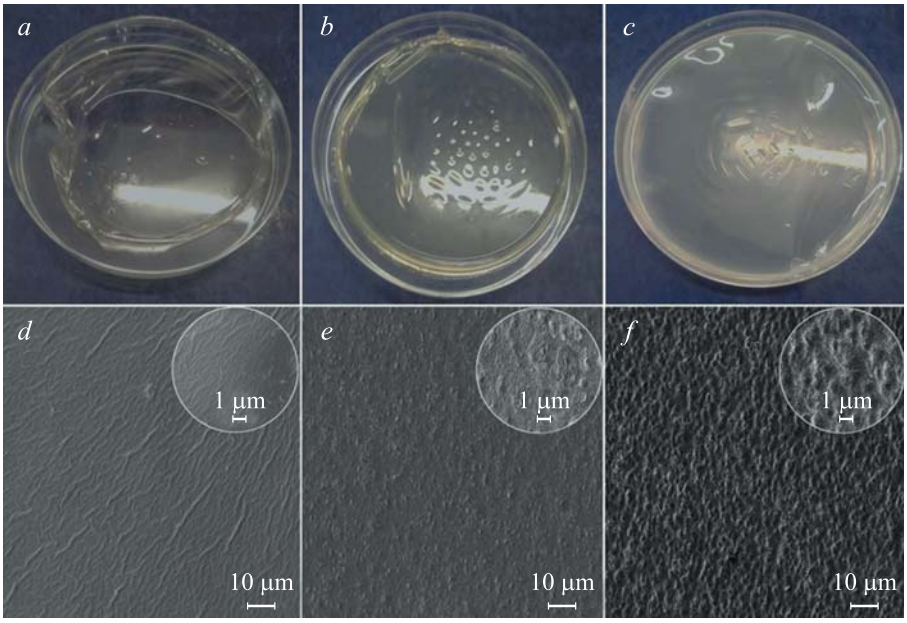

Fig. 2. Films obtained from sodium alginate plasticized with glycerol and PEG 400 and their respective SEM images with a magnification of 1.00 KX (10 μm) and 5.00 KX (1 μm): NaAlgCG9P1 (*a*, *d*), NaAlgCG7P3 (*b*, *e*) and NaAlgCG5P5 (*c*, *f*)

Table 2

Values of thickness, transmittance at 600 nm, opacity, and moisture content of the films obtained at different proportions of plasticizers

Film	Thickness, μm	T_{600}, %	Opacity, AU — nm · mm^{-1}	Water content, g (H_2O) g^{-1} (d.S.)
NaAlgCG9P1	173.43 ± 4.18	90.18	0.26	0.8975 ± 0.2719
NaAlgCG7P3	102.92 ± 2.59	64.93	1.82	0.7654 ± 0.0942
NaAlgCG5P5	164.57 ± 2.08	19.33	4.34	0.3145 ± 0.0702

NB. T_{600} (%) is percent of transmittance at 600 nm.

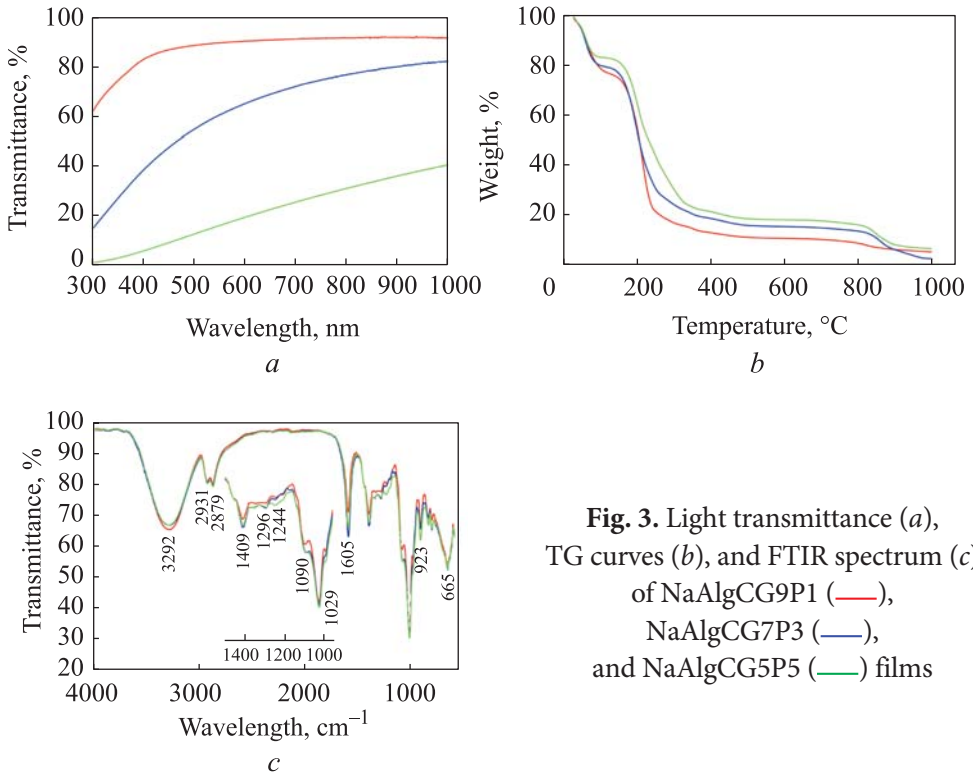

Fig. 3. Light transmittance (*a*), TG curves (*b*), and FTIR spectrum (*c*) of NaAlgCG9P1 (——), NaAlgCG7P3 (——), and NaAlgCG5P5 (——) films

Figure 3, *b* presents the TG curves of the films whose mass losses were assigned to the thermal events of dehydration, film degradation, polymer degradation, and carbonization [28]. The larger amount of glycerol in the mixture of plasticizer resulted in an increased mass loss during dehydration step, due to the higher hydrophobicity resulting from the presence of hydroxylated glycerol in the samples [29]. The thermal events and the mass loss with their respective temperature ranges of these films are summarized in Table 3.

Table 3

Mass loss values from TGA of NaAlgCG9P1, NaAlgCG7P3, and NaAlgCG5P5 films

Film	Weight, mg	Thermal event	ΔT, °C	Mass loss, %
NaAlgCG9P1	5.176	Dehydration	22.0–120.3	22.8
		Film degradation	120.3–321.3	61.1
		Polymer degradation	321.3–615.0	5.10
		Carbonization	615.0–989.5	5.41
		Carbonaceous residue	989.5	5.59
NaAlgCG7P3	5.051	Dehydration	21.0–108.2	20.3
		Film degradation	108.2–378.0	61.0
		Polymer degradation	378.0–616.0	3.76
		Carbonization	616.0–991.5	12.92
		Carbonaceous residue	991.5	2.02
NaAlgCG5P5	5.470	Dehydration	22.1–105.0	17.0
		Film degradation	105.0–379.4	62.0
		Polymer degradation	379.4–630.3	3.79
		Carbonization	630.3–990.1	11.58
		Carbonaceous residue	990.1	5.63

The FTIR spectra of the films prepared with different ratios of the plasticizers are presented in Fig. 3, *c*. The bands at 2931 and 2879 cm^{-1} are associated with C–H stretching [30]. On the other hand, the increase of PEG 400 generates more intense bands at 1605, 1409, 1244, and 1090 cm^{-1}, which correspond to the asymmetric and symmetric stretching of the carboxylate [31] and C–OH and C–O–C stretches [32]; respectively. However, the increase of glycerol in the mixture of plasticizers increases the band corresponding to the hydroxyl group (–OH) (3292 cm^{-1}), as well as those from water. Therefore, it is assumed that the hydrogen bonds between water and sodium alginate were weakened due to the higher water-plasticizer affinity. Being partially replaced by the relatively weaker hydrogen bonds between the polar groups of the plasticizers and those corresponding to the polymeric matrix [33].

Second stage. Three films composed of sodium alginate with carrageenan (κ-carrageenan and/or ι-carrageenan) and plasticized with glycerol/PEG 400 in a 9:1 ratio were prepared. The films were called NaAlgCG9P1k (Fig. 4, *a*), NaAlgCG9P1i (Fig. 4, *b*), and NaAlgCG9P1ki (Fig. 4, *c*). The SEM images

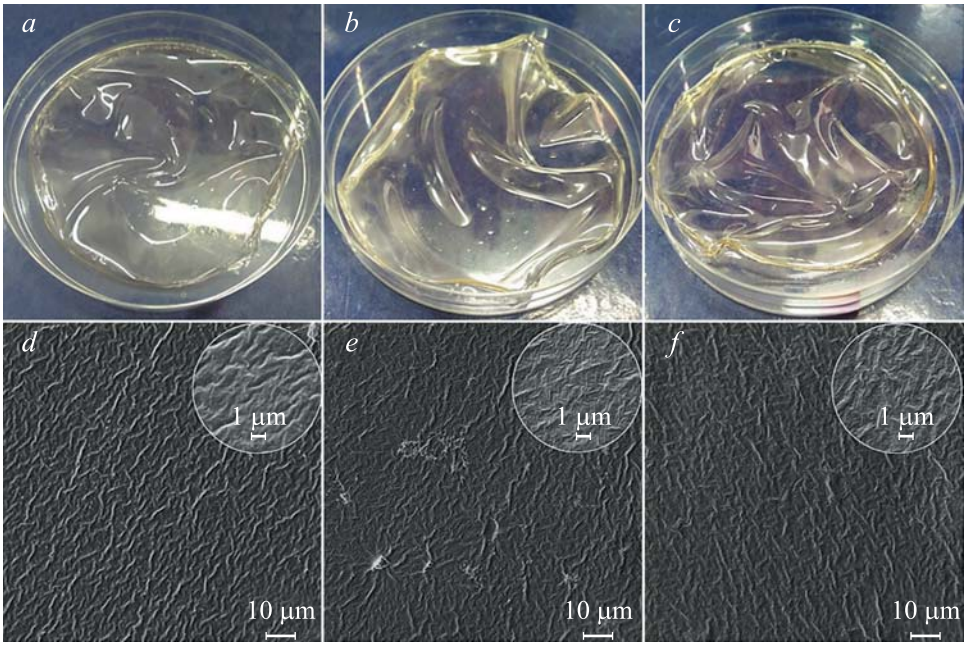

Fig. 4. Sodium alginate/carrageenan/glycerol/PEG 400 composite films, and their respective SEM images at 1.00 KX (10 μm) and 5.00 KX (1 μm) magnification: NaAlgCG9P1k (*a*, *d*), NaAlgCG9P1i (*b*, *e*) and NaAlgCG9P1ki (*c*, *f*)

(Fig. 4, *d*, *f*, and *g*) show that the surface of these films is rougher and more heterogeneous compared to the film containing only sodium alginate and the 9:1 mixture of plasticizers (see Fig. 2, *d*). For example, at a scale of 1 μm, the surface of the NaAlgCG9P1k film (see Fig. 4, *d*) has wide slits, and the NaAlgCG9P1i film (Fig. 4, *e*) has a greater number of thin striations on the surface. However, the film NaAlgCG9P1ki (see Fig. 4, *f*) presents aggregates not as refined as the film containing only ι-carrageenan. This is due to the rapid gelation of ι-carrageenan, which is induced by temperature and/or the presence of salts [34].

The presence of ι-carrageenan in the films leads to a greater hydrophilic character represented by the greater mass loss during the dehydration process, and it showed a higher amount of carbonaceous residues compared to the film prepared with κ-carrageenan. Sulfate groups are highly polar, which could increase the hydrophilic character and induce the thermostability in the films. This possibility can be supported by the fact that the residual weights in neat κ-, and ι-carrageenans are 16 and 21 %, respectively [35–37] (Fig. 5, *a*). The thermal events and the mass loss with their respective temperature intervals of these films are summarized in Table 4.

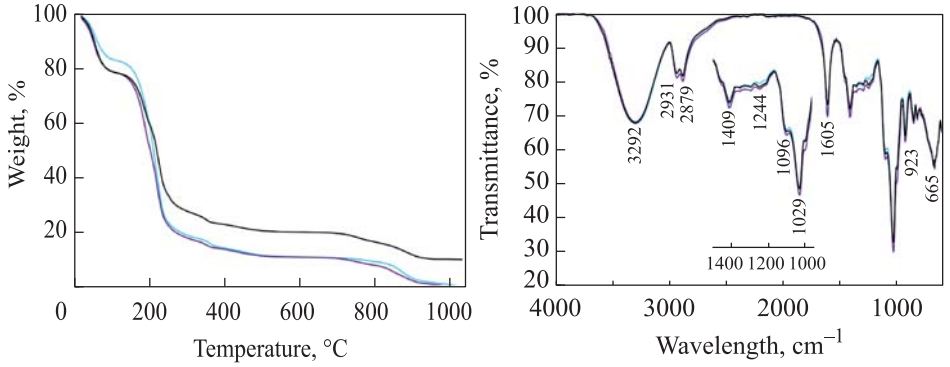

a *b*

Fig. 5. TG curves (*a*) and FTIR spectrum (*b*) of NaAlgCG9P1k (——), NaAlgCG9P1i (——), and NaAlgCG9P1ki (——) films

Table 4

Mass loss values from TGA of NaAlgCG9P1k, NaAlgCG9P1i, and NaAlgCG9P1ki films

Film	Weight, mg	Thermal event	Δ*T*, °C	Mass loss, %
NaAlgCG9P1k	5.131	Dehydration	21.1–113.9	16.4
		Film degradation	113.9–581.9	72.1
		Polymer degradation	581.9–909.5	9.32
		Carbonization	909.5–991.3	1.21
		Carbonaceous residue	991.3	0.97
NaAlgCG9P1i	4.740	Dehydration	22.2–109.0	20.2
		Film degradation	109.0–594.8	67.5
		Polymer degradation	594.8–901.5	9.71
		Carbonization	901.5–992.2	1.28
		Carbonaceous residue	992.2	1.31
NaAlgCG9P1ki	5.187	Dehydration	20.9–115.5	21.1
		Film degradation	111.5–599.7	59.0
		Polymer degradation	599.7–937.0	10.01
		Carbonization	937.0–992.4	0.13
		Carbonaceous residue	992.4	9.76

In the FTIR spectra (Fig. 5, *b*), no additional bands are evident concerning the FTIR spectrum of the NaAlgCG9P1 film (see Fig. 3, *c*), which was used as base film; however, the bands at 1029 and 923 cm^{-1} are associated with the S = O vibrational mode [38] and the C–O–C stretching of 3,6-anhydro-D-galactose [39, 40] of carrageenan derivatives, respectively. Therefore, it is assumed that the additional sulfate ester group that contains the ι-carrageenan

interacts with a greater number of –OH groups, forming hydrogen bonds and, with it, greater interaction with the polymeric matrix of sodium alginate.

Third stage. Figure 6, *a* shows the NaAlgCG9P1kiA film, and the SEM image of the film's surface is depicted in Fig. 6, *b*. In the SEM image, the film loaded with AVG presents a homogeneous surface compared to the surface of the NaAlgCG9P1ki film (see Fig. 4, *f*); this is because ethanol positively impacts the homogeneity and visual appearance of alginate films. Since sodium alginate is not soluble in ethanol, a packed polymer matrix was formed, thus the degree of swelling of the films was decreased and less shrinkage was obtained during the film drying process [41].

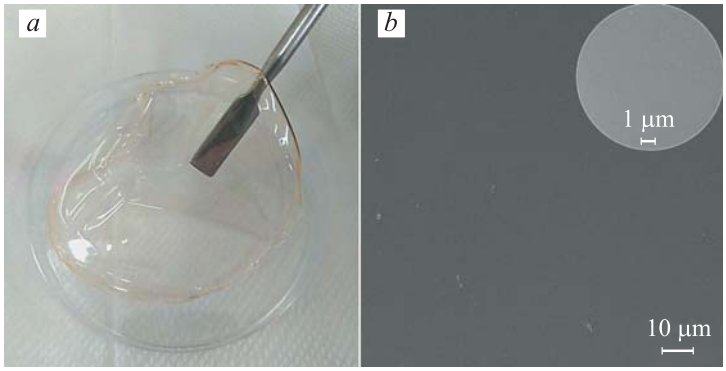

Fig. 6. NaAlgCG9P1kiA film (*a*), SEM image at 1.00 KX (10 μm) and 5.00 KX (1 μm) magnification (*b*)

Figure 7, *a* shows the XRD diffractograms of the NaAlgCG9P1, NaAlgCG9P1ki, and NaAlgCG9P1kiA films, which offer a diffraction peak close to 21° in the diffraction pattern corresponding to the mannuronate unit of sodium alginate [42]. The crystallinity index of the films was calculated using the ratio of the crystalline region and the total diffraction area. The NaAlgCG9P1 film has a crystallinity percentage of 23.75 % due to the interaction between the plasticizers and the NaAlg polymer matrix. This indicates that the microstructure of this film is homogeneous [33]. The NaAlgCG9P1ki film presents a crystallinity percentage of 25.97 %; however, loading an ethanolic AVG solution causes the crystallinity of the NaAlgCG9P1kiA film to be 45.73 %. This can be attributed to the polarity of the ethanol molecules, which rearranges the intermolecular hydrogen bonds within the polymeric matrix [43].

Figure 7, *b* shows the TG curve (TGA) of the NaAlgCG9P1kiA film, which offers a higher percentage of mass loss during the dehydration process (25.6 %) compared to the NaAlgCG9P1ki film (see Table 4). This is due to the increase in polar groups in the ethanolic solution of AVG. On another hand, the presence

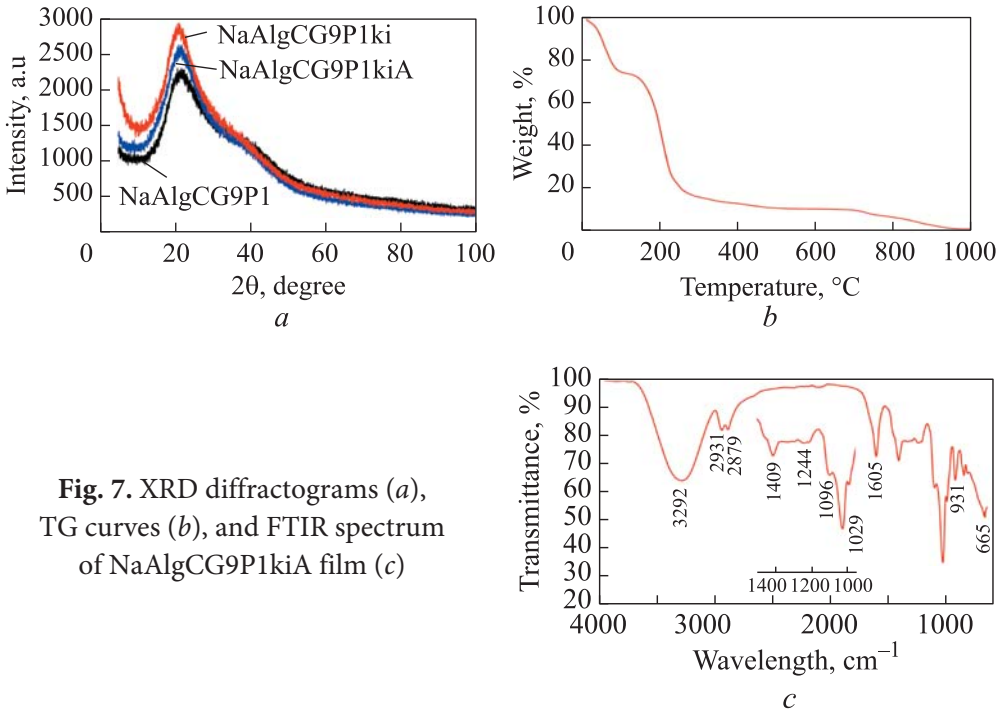

Fig. 7. XRD diffractograms (*a*), TG curves (*b*), and FTIR spectrum of NaAlgCG9P1kiA film (*c*)

of AVG in the composite seems to interfere in the interchain interactions and leaded to a degradation profile similar to those observed for the individual carrageenan, with higher polymer degradation that resulted in a low carbonaceous residue. The thermal events and the mass loss with their respective temperature intervals of this film are summarized in Table 5.

Table 5

Mass loss values from thermogravimetric analysis of NaAlgCG9P1kiA films, weight 6.474 mg

Thermal event	ΔT, °C	Mass loss, %
Dehydration	18.9–117.3	25.6
Film degradation	117.3–318.2	58.8
Polymer degradation	318.2–566.0	4.87
Carbonization	566.0–992.3	9.59
Carbonaceous residue	992.3	1.14

The FTIR spectrum of the NaAlgCG9P1kiA film (Fig. 7, *c*) does not show the disappearance of bands concerning the FTIR spectrum of the NaAlgCG9P1ki film (see Fig. 4, *b*), so it is assumed that there are no structural changes in the polymer matrices.

Kinetic behavior of aminoethoxyvinylglycine release. The AVG release profiles (Fig. 8) show that at 10 °C the film released 18.89 mg · L^{-1} (94.45 %) of AVG, while at 25 °C only 8.64 mg · L^{-1} (43.2 %) was released, which suggests that this system has a faster release response at low temperatures. Table 6 shows the values of the correlation coefficient R^2 and the diffusion exponent n calculated from Eq. (1), (2). The Korsmeyer — Peppas model has a higher R^2 value than the Higuchi model in both release profiles, so it better describes the release of AVG. Additionally, the value of n is greater than 0.5 and less than 1.0, so it is assumed that the release is carried out by an anomalous or non-Fickian diffusion [44].

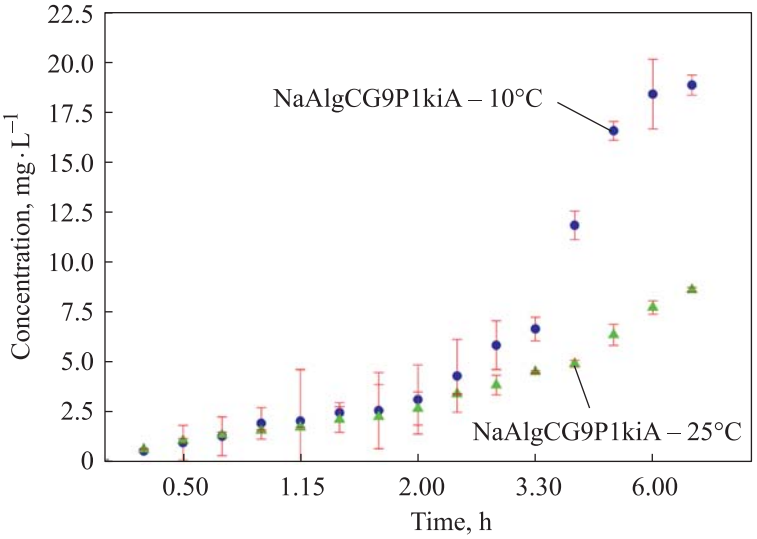

Fig. 8. Release profiles at 10 and 25 °C of AVG

Table 6

Kinetic parameters obtained by the method of Higuchi and Korsmeyer — Peppas for NaAlgCG9P1kiA film

Temperature, °C	Higuchi	Korsmeyer — Peppas	
	R^2	n	R^2
10	0.8211	0.9513	0.9367
25	0.9322	0.6585	0.9628

Conclusion. Thus, we can conclude that the 9:1 w · w^{-1} ratio of glycerol and PEG 400 makes it possible to obtain sodium alginate films with a homogeneous surface, lower opacity, and higher moisture content. The mixture of κ-carra-

geenan and ι-carrageenan reduces the heterogeneity on the surface of the film and the loss of mass during the degradation process in the TG, compared to the films containing the carrageenans separately. Adding an ethanolic solution of AVG generates a positive impact on the film's surface, and the ethanolic solution is a good release medium for AVG release at low temperatures.

REFERENCES

[1] de Oliveira Filho J.G., Rodrigues J.M., Valadares A.C.F., et al. Active food packaging: alginate films with cottonseed protein hydrolysates. *Food Hydrocoll.*, 2019, vol. 92, pp. 267–275. DOI: https://doi.org/10.1016/j.foodhyd.2019.01.052

[2] Łupina K., Kowalczyk D., Kazimierczak W. Gum arabic/gelatin and water-soluble soy polysaccharides/gelatin blend films as carriers of astaxanthin — a comparative study of the kinetics of release and antioxidant properties. *Polymers*, 2021, vol. 13, iss. 7, art. 1062. DOI: https://doi.org/10.3390/polym13071062

[3] Li J., Xiang H., Zhang Q., et al. Polysaccharide-based transdermal drug delivery. *Pharmaceuticals*, 2022, vol. 15, iss. 5, art. 602. DOI: https://doi.org/10.3390/ph15050602

[4] Marangoni L., Rodrigues P.R., da Silva R.G., et al. Sustainable packaging films composed of sodium alginate and hydrolyzed collagen: preparation and characterization. *Food Bioprocess Technol.*, 2021, vol. 14, no. 12, pp. 2336–2346.
DOI: https://doi.org/10.1007/s11947-021-02727-7

[5] Malviya R., Tyagi A., Fuloria S., et al. Fabrication and characterization of chitosan — tamarind seed polysaccharide composite film for transdermal delivery of protein/peptide. *Polymers*, 2021, vol. 13, iss. 9, art. 1531.
DOI: https://doi.org/10.3390/polym13091531

[6] Fan Y., Yang J., Duan A., et al. Pectin/sodium alginate/xanthan gum edible composite films as the fresh-cut package. *Int. J. Biol. Macromol.*, 2021, vol. 181, pp. 1003–1009. DOI: https://doi.org/10.1016/j.ijbiomac.2021.04.111

[7] Hasan N., Cao J., Lee J., et al. Development of clindamycin-loaded alginate/pectin/hyaluronic acid composite hydrogel film for the treatment of MRSA-infected wounds. *J. Pharm. Investig.*, 2021, vol. 51, no. 5, pp. 597–610.
DOI: https://doi.org/10.1007/s40005-021-00541-z

[8] Fahmy H.M., Aly A.A., Sayed S.M., et al. K-carrageenan/Na-alginate wound dressing with sustainable drug delivery properties. *Polym. Adv. Met. Technol.*, 2021, vol. 32, iss. 4, pp. 1793–1801. DOI: https://doi.org/10.1002/pat.5218

[9] Chen J., Wu A., Yang M., et al. Characterization of sodium alginate-based films incorporated with thymol for fresh-cut apple packaging. *Food Control*, 2021, vol. 126, art. 108063. DOI: https://doi.org/10.1016/j.foodcont.2021.108063

[10] Anis A., Pal K., Al-Zahrani S.M. Essential oil-containing polysaccharide-based edible films and coatings for food security applications. *Polymers*, 2021, vol. 13, iss. 4, art. 575. DOI: https://doi.org/10.3390/polym13040575

[11] Pacheco E., Ruiz R., Veiga M. Carrageenan: drug delivery systems and other biomedical applications. *Mar. Drugs*, 2020, vol. 18, iss. 1, art. 583.
DOI: https://doi.org/10.3390/md18110583

[12] de Lima Barizão C., Crepaldi M.I., de Oliveira O.S. Jr., et al. Biodegradable films based on commercial κ-carrageenan and cassava starch to achieve low production costs. *Int. J. Biol. Macromol*., 2020, vol. 165A, pp. 582–590.
DOI: https://doi.org/10.1016/j.ijbiomac.2020.09.150

[13] Brenner T., Tuvikene R., Parker A., et al. Rheology and structure of mixed kappa-carrageenan/iota-carrageenan gels. *Food Hydrocoll*., 2014, vol. 39, pp. 272–279.
DOI: https://doi.org/10.1016/j.foodhyd.2014.01.024

[14] Bharti S.K., Pathak V., Arya A., et al. Packaging potential of *Ipomoea batatas* and κ-carrageenan biobased composite edible film: its rheological, physicomechanical, barrier and optical characterization. *J. Food Process. Preserv*., 2021, vol. 45, iss. 2, art. e15153. DOI: https://doi.org/10.1111/jfpp.15153

[15] Guo S., Fu Z., Sun Y., et al. Effect of plasticizers on the properties of potato flour films. *Starch*, 2022, vol. 74, iss. 1-2, art. 2100179.
DOI: https://doi.org/10.1002/star.202100179

[16] de Oliveira A.C.S., Ugucioni J.C., Borges S.V. Effect of glutaraldehyde/glycerol ratios on the properties of chitosan films. *J. Food Process. Preserv*., 2021, vol. 45, iss. 1, art. e15060. DOI: https://doi.org/10.1111/jfpp.15060

[17] Šešlija S., Nešić A., Ružić J., et al. Edible blend films of pectin and poly(ethylene glycol): Preparation and physico-chemical evaluation. *Food Hydrocoll*., 2018, vol. 77, pp. 494–501. DOI: https://doi.org/10.1016/j.foodhyd.2017.10.027

[18] Lecomte F., Siepmann J., Walther M., et al. Polymer blends used for the aqueous coating of solid dosage forms: importance of the type of plasticizer. *J. Control Release*, 2014, vol. 99, iss. 1, pp. 1–13. DOI: https://doi.org/10.1016/j.jconrel.2004.05.011

[19] Norcino L.B., Mendes J.F., Natarelli C.V.L., et al. Pectin films loaded with copaiba oil nanoemulsions for potential use as bio-based active packaging. *Food Hydrocoll*., 2020, vol. 106, art. 105862. DOI: https://doi.org/10.1016/j.foodhyd.2020.105862

[20] Siripatrawan U., Kaewklin P. Fabrication and characterization of chitosan-titanium dioxide nanocomposite film as ethylene scavenging and antimicrobial active food packaging. *Food Hydrocoll*., 2018, vol. 84, pp. 125–134.
DOI: https://doi.org/10.1016/j.foodhyd.2018.04.049

[21] Liu J., Islam M.T., Sherif S.M. Effects of aminoethoxyvinylglycine (AVG) and 1-methylcyclopropene (1-MCP) on the pre-harvest drop rate, fruit quality, and stem-end splitting in 'Gala' apples. *Horticulturae*, 2022, vol. 8, no. 12, art. 1100.
DOI: https://doi.org/10.3390/horticulturae8121100

[22] Kent Peters N., Crist-Estes D.K. Nodule formation is stimulated by the ethylene inhibitor aminoethoxyvinylglycine. *Plant Physiol*., 1989, vol. 91, iss. 2, pp. 690–693. DOI: https://doi.org/10.1104/pp.91.2.690

[23] Higuchi T. Mechanism of sustained-action medication. Theoretical analysis of rate of release of solid drugs dispersed in solid matrices. *J. Pharm. Sci*., 1963, vol. 52, iss. 12, pp. 1145–1149. DOI: https://doi.org/10.1002/jps.2600521210

[24] Korsmeyer R.W., Gurny R., Doelker E., et al. Mechanisms of solute release from porous hydrophilic polymers. *Int. J. Pharm*., 1983, vol. 15, iss. 1, pp. 25–35. DOI: https://doi.org/10.1016/0378-5173(83)90064-9

[25] Saberi B., Chockchaisawasdee S., Golding J.B., et al. Physical and mechanical properties of a new edible film made of pea starch and guar gum as affected by glycols, sugars and polyols. *Int. J. Biol. Macromol*., 2017, vol. 104, part A, pp. 345–359. DOI: https://doi.org/10.1016/j.ijbiomac.2017.06.051

[26] Cao N., Fu Y., He J. Preparation and physical properties of soy protein isolate and gelatin composite films. *Food Hydrocoll*., 2007, vol. 21, iss. 7, pp. 1153–1162. DOI: https://doi.org/10.1016/j.foodhyd.2006.09.001

[27] Ahmed A., Boateng J. Calcium alginate-based antimicrobial film dressings for potential healing of infected foot ulcers. *Ther. Deliv*., 2018, vol. 9, no. 3, pp. 185–204. DOI: https://doi.org/10.4155/tde-2017-0104

[28] Zia T., Usman M., Sabir A., et al. Development of inter-polymeric complex of anionic polysaccharides, alginate/k-carrageenan bio-platform for burn dressing. *Int. J. Biol. Macromol*., 2020, vol. 157, pp. 83–95. DOI: https://doi.org/10.1016/j.ijbiomac.2020.04.157

[29] Basiak E., Lenart A., Debeaufort F. How glycerol and water contents affect the structural and functional properties of starch-based edible films. *Polymers*, 2018, vol. 10, iss. 4, art. 412. DOI: https://doi.org/10.3390/polym10040412

[30] Kongjao S., Damronglerd S., Hunsom M. Purification of crude glycerol derived from waste used-oil methyl ester plant. *Korean J. Chem. Eng*., 2010, vol. 27, no. 3, pp. 944–949. DOI: https://doi.org/10.1007/s11814-010-0148-0

[31] Zheng H., Yang J., Han S. The synthesis and characteristics of sodium alginate/graphene oxide composite films crosslinked with multivalent cations. *J. Appl. Polym. Sci*., 2016, vol. 133, iss. 27, art. 43616. DOI: https://doi.org/10.1002/app.43616

[32] Khairuddin, Pramono E., Utomo S.B., et al. FTIR studies on the effect of concentration of polyethylene glycol on polimerization of shellac. *J. Phys.: Conf. Ser*., 2016, vol. 776, art. 012053. DOI: https://doi.org/10.1088/1742-6596/776/1/012053

[33] Gao C., Pollet E., Avérous L. Properties of glycerol-plasticized alginate films obtained by thermo-mechanical mixing. *Food Hydrocoll*., 2017, vol. 63, pp. 414–420. DOI: https://doi.org/10.1016/j.foodhyd.2016.09.023

[34] Paula G.A., Benevides N.M.B., Cunha A.P., et al. Development and characterization of edible films from mixtures of κ-carrageenan, ι-carrageenan, and alginate. *Food Hydrocoll*., 2015, vol. 47, pp. 140–145. DOI: https://doi.org/10.1016/j.foodhyd.2015.01.004

[35] Campo V.L., Kawano D.F., Silva D.B., et al. Carrageenans: biological properties, chemical modifications and structural analysis — a review. *Carbohydr. Polym*., 2009, vol. 77, iss. 2, pp. 167–180. DOI: https://doi.org/10.1016/j.carbpol.2009.01.020

[36] Bantang J.P., Bigol U.G., Camacho D.H. Gel and film composites of silver nanoparticles in κ-, ι-, and λ-carrageenans: one-pot synthesis, characterization, and bioactivities. *BioNanoSci*., 2021, vol. 11, no. 1, pp. 53–66.
DOI: https://doi.org/10.1007/s12668-020-00806-1

[37] Mohamadnia Z., Zohuriaan-Mehr M., Kabiri K., et al. Ionically cross-linked carrageenan-alginate hydrogel beads. *J. Biomater. Sci. Polym. Ed*., 2008, vol. 19, iss. 1, pp. 47–59. DOI: https://doi.org/10.1163/156856208783227640

[38] Karthikeyan S., Selvasekarapandian S., Premalatha M., et al. Proton-conducting I-carrageenan-based biopolymer electrolyte for fuel cell application. *Ionics*, 2017, vol. 23, no. 10, pp. 2775–2780. DOI: https://doi.org/10.1007/s11581-016-1901-0

[39] Ghani N.A.A., Othaman R., Ahmad A., et al. Impact of purification on iota-carrageenan as solid polymer electrolyte. *Arab. J. Chem*., 2019, vol. 12, iss. 3, pp. 370–376. DOI: https://doi.org/10.1016/j.arabjc.2018.06.008

[40] Perumal P., Selvin P.C. Red algae-derived k-carrageenan-based proton-conducting electrolytes for the wearable electrical devices. *J. Solid State Electrochem*., 2020, vol. 24, no. 11, pp. 2249–2260. DOI: https://doi.org/10.1007/s10008-020-04724-w

[41] Li J., He J., Huang Y., et al. Improving surface and mechanical properties of alginate films by using ethanol as a co-solvent during external gelation. *Carbohydr. Polym*., 2015, vol. 123, pp. 208–216. DOI: https://doi.org/10.1016/j.carbpol.2015.01.040

[42] Sundarrajan P., Eswaran P., Marimuthu A., et al. One pot synthesis and characterization of alginate stabilized semiconductor nanoparticles. *Bull. Korean Chem. Soc*., 2012, vol. 33, iss. 10, pp. 3218–3224.
DOI: https://doi.org/10.5012/BKCS.2012.33.10.3218

[43] Puerta M., Peresin M.S., Restrepo-Osorio A. Effects of chemical post-treatments on structural and physicochemical properties of silk fibroin films obtained from silk fibrous waste. *Front. Bioeng. Biotechnol*., 2020, vol. 8, art. 523949.
DOI: https://doi.org/10.3389/fbioe.2020.523949

[44] Bataglioli R.A., Taketa T.B., Rocha Neto J.B.M., et al. Analysis of pH and salt concentration on structural and model-drug delivery properties of polysaccharide-based multilayered films. *Thin Solid Films*, 2019, vol. 685, pp. 312–320.
DOI: https://doi.org/10.1016/j.tsf.2019.06.039

Villacrés Nelson Adrián — Post-Graduate Student, Faculty of Sciences, National University of Engineering (Tupac Amaru av. 210, Rimac, Lima, Peru).

Cavalheiro Éder Tadeu Gomes — Dr. Sc., Professor, São Carlos Institute of Chemistry, University of São Paulo (São Carlos, São Paulo CEP 13566-590, Brazil).

Ferreira Ana García — Dr. Sc., São Carlos Institute of Chemistry, University of São Paulo (São Carlos, São Paulo CEP 13566-590, Brazil).

Venâncio Tiago — Dr. Sc., Professor, Nuclear Magnetic Resonance Laboratory, Department of Chemistry, Federal University of São Carlos (São Carlos, São Paulo, Brazil).

Alarcon Hugo — Dr. Sc., Professor, Faculty of Sciences, National University of Engineering (Tupac Amaru av. 210, Rimac, Lima, Peru).

Valderrama Ana — Dr. Sc., Professor, Faculty of Sciences, National University of Engineering (Tupac Amaru av. 210, Rimac, Lima, Peru).

Please cite this article as:

Villacrés N.A., Cavalheiro É.T.G., Ferreira A.P.G., et al. Preparation and characterization of biocomposite films of sodium alginate/kappa-carrageenan/iota-carrageenan loaded with aminoethoxyvinylglycine. *Herald of the Bauman Moscow State Technical University, Series Natural Sciences*, 2023, no. 4 (109), pp. 175–193.
DOI: https://doi.org/10.18698/1812-3368-2023-4-175-193